Polymer Bulletin 59, 381–390 (2007)
DOI 10.1007/s00289-007-0773-x

Polymer Bulletin

Comparison of tensile fracture morphologies among various polyacrylonitrile-based carbon fibers

Minxia Ji[1, 2] (✉), Chengguo Wang[1], Yujun Bai[1], Meijie Yu[1], Yanxiang Wang[1]

[1]Key Laboratory of Liquid Structure and Heredity of Materials, Ministry of Education, Shandong University, Jinan 250061, China
[2]Carbon Fiber Engineering Research Center of Shandong Province, College of Materials Science and Engineering, Shandong University, Jinan 250061, China
E-mail: ji_minxia@163.com

Received: 11 March 2007 / Accepted: 15 April 2007
Published online: 27 April 2007 –

Summary

Tensile fracture morphologies of three kinds of polyacrylonitrile-based carbon fibers were investigated by scanning electron microscope and high resolution transmission electron microscope. Homogeneous and granular texture could be observed in cross sections of all these three carbon fibers. There is a void up to 1μm in diameter in fracture surface of T1, which limits its compactness and tensile strength. Apart from homogeneous texture, linear and fan-shaped morphology are found on surface of T300 and T700, respectively. No core-sheath structure was found in these specimens. Misoriented crystallites are also found from HRTEM images in the transverse sections of T1, T300 and T700, which initiate fiber tensile failure. The tensile fracture mechanism and the implication of the fiber structure under tensile force were also elucidated. T700 has the smallest interplanar spacing, the highest degree of graphitization and the highest crystallinity among three carbon fibers.

Introduction

Because of their unique properties such as high strength, high modulus and light weight, polyacrylonitrile (PAN)-based carbon fibers have been widely used as reinforced materials in the fields of aerospace and other high technology industries [1]. The theoretical tensile strength of single crystal of graphite is 180 GPa, the highest of all the materials known. Though in the past decades there have been very significant improvements in the tensile strength of carbon fibers, at present commercial high strength carbon fibers have a maximum strength of 7.02 GPa, only 3.9 percent of theoretical value [2]. So, there still seems to be a lot of room for improving the properties of carbon fibers. The key is to unambiguously understand the tensile fracture mechanism and the implication of fiber structure under tensile force, and to find out the relationship between structure and tensile strength of fibers, because fracture surfaces of fibers exhibit morphological features related to variations in the physical properties.

A lot of researches have been done on the properties and morphology of carbon fibers [3-9], but most of the previous work has been confined to the single type carbon fiber,

whereas this work mainly compares differences of tensile fracture morphologies among various PAN-based carbon fibers, and gets better understanding of relationship between structure and tensile strength of fibers. In this study, scanning electron microscopy (SEM) and high resolution transmission electron microscopy (HRTEM) were used for insight into the morphological features. Based on the experimental results, the tensile fracture mechanism of carbon fibers was discussed.

Experimental

Materials

Three kinds of polyacrylonitrile-based carbon fibers with different tensile strengths (named as T1, T300, T700, respectively) were selected in this study. T1 was produced in our laboratory. The conversion from PAN solution to carbon fibers undergoes three indispensable process: spinning, thermal stabilization, and carbonization. For wet spinning precursor fibers of T1, a 21 wt.% copolymer was prepared in dimethylsulfoxide (DMSO) of acrylonitrile/itaconic acid (AN/IA 99/1 wt.%) using azodiisobutyronitrile (AIBN) as initiator. The precursor fibers of T1 with 1000 filaments in each single tow have an average titre of 0.98 dtex, and tensile strength of 7.36 cN/dtex. A self-designed continuous carbon fiber production line as shown in Figure 1 was used for thermal stabilization and closely linked carbonization of precursor fibers. The line is composed of two thermal stabilization furnaces that each have five separate temperature zones, two carbonization furnaces and eight sets of stretching equipments. The precursor fibers were thermal stabilized in a purified air atmosphere at 195-275°C under a 5% stretching ratio. Subsequently, the oxidized fibers were subjected to low-temperature carbonization in a pure nitrogen atmosphere from 350-600°C under a 1.5% stretching ratio, and high-temperature carbonization also in a pure nitrogen atmosphere from 1280-1400°C under a 4% stretching ratio to obtain the resulting carbon fibers. Another two type carbon fibers of T300 and T700 were commercially supplied by Toray. The related properties are listed in Table 1.

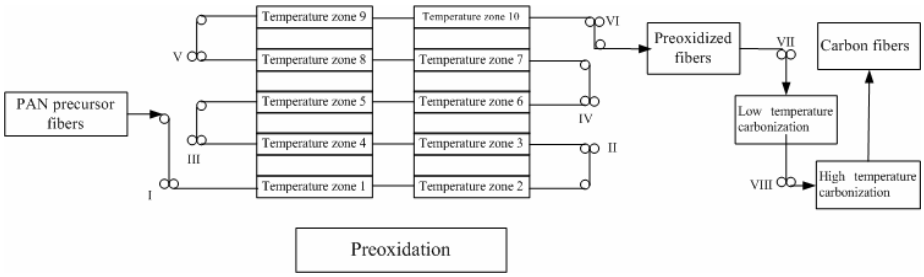

Figure 1 Scheme of carbon fiber production line with (I~VIII) stretching rollers

Table 1 Some properties of selected PAN-based carbon fibers

Sample	Density (g/cm^3)	Tensile Strength (GPa)	Young's Modulus (GPa)	Elongation at break (%)	Crystallinity (%)	Interplanar Spacing (Å)
T1	1.75	3.50	200	1.70	21.8	3.432
T300	1.76	3.54	231	1.50	29.6	3.427
T700	1.80	4.92	231	2.10	31.6	3.425

Measurements

The density of carbon fibers was obtained at 25°C by a density gradient column method in a mixture of n-heptane and ethylene bromide.
Carbon fibers were impregnated with epoxy resin and cured at 120°C. Then the samples were drawn to failure by CMT4204 tensile test machine (Shenzhen Sans Testing Machine Co., Ltd, Shenzhen, China).
A Rigaku D/max-rc X-ray diffractometer with Ni-filtered Cukα radiation (λ=0.15418nm) was used to determine the structural parameters of carbon fibers. The scanning rate is 4°/min with a scanning step of 0.02°. The crystallinity (C) of fibers is measured by Hinrichen's method [10]:

$$C = \frac{A_c}{A_a + A_c} \times 100\% \quad (1)$$

where A_c is the area under the crystalline diffraction peaks and A_a is the area of amorphous zone.
Fracture morphologies of carbon fibers were topographically examined and photographed using JEC-560 scanning electron microscope (JEOL, Japan). Prior to examination, the specimens were coated with carbon to get a better image.
Carbon fibers were embedded with epoxy resin and solidified. Then ultrathin transverse sections were cut respectively on a Reichert-Jung Ultracut E Ultramicrotome (Austria) using a diamond knife and collected on copper microgrids covered with carbon film. The transverse sections were examined using a Philips Tecnai 20U-Twin high resolution transmission electron microscope (America) at an accelerating voltage of 200 kV.

Results and Discussion

SEM analysis of fracture morphology

Figure 2 is the SEM images of the fracture morphology of T1. From Figure 2(a) and 2(b), the fracture morphologies show rough and granular texture. The diameter of the granules is in the range of 100-250nm, which accords with the diameter of fibrils [11-12], so we can conclude that granules are the fracture end of fibrils. In the transverse direction the granules distribute randomly. This is easily understood from the precursor [13]. Chain-like molecules are present when PAN is spun. Subsequent cyclization into polyaromatic entities will thus occur following an axial orientation due to the previous alignment of the chain-like molecules, but will occur randomly in the transverse direction, providing the well-known random transverse texture.
Figure 2(c) is another SEM image of T1 showing a void about 1 μm in diameter. The tensile fracture of T1 may originate from the void. The present of void is reflected in the density, which is the lowest in the three kinds of carbon fibers as shown in Table 1. Larger density matches well with higher compactness, and higher compactness represents that carbon fibers have fewer flaws and higher tensile strength. Voids should also be examined as a possible source of the tensile fracture. It is suggested that by reducing void size and number, carbon fibers with a high tensile strength will be obtained.

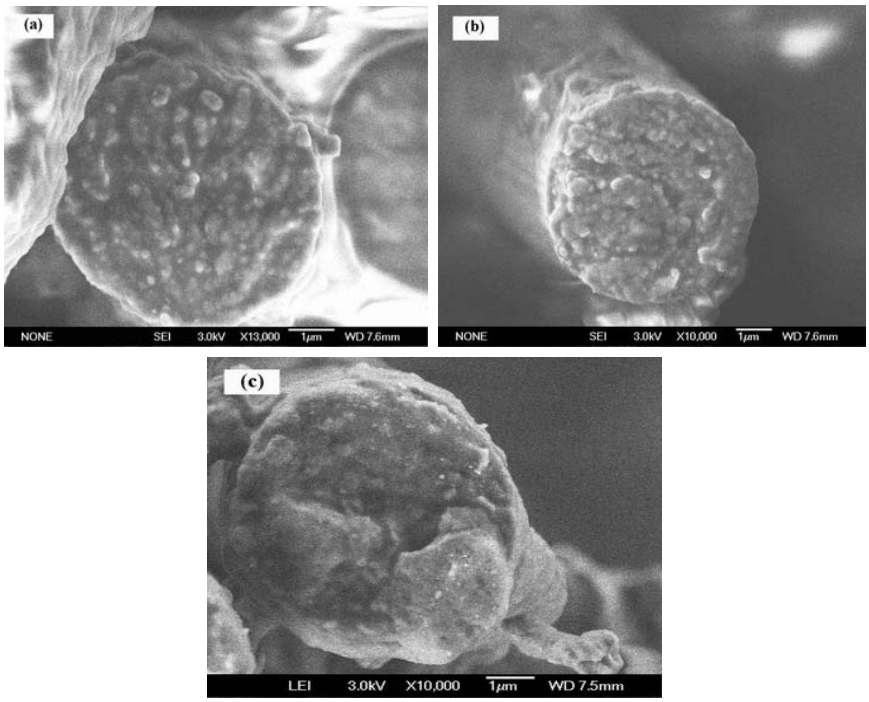

Figure 2 SEM images of the fracture morphology of T1

Figure 3 displays the fracture morphologies of T300 from Toray. It can be seen from Figure 3(a) and 3(b) that the grainy and homogeneous textures are consistent with those observed in T1. Compared with T1, T300 with the diameter of granules in the range of 100-300nm has a rather poorly defined granular and rough texture.

Figure 3(c) is another fracture surface of T300. In the center of cross sections, the granules are distributed in a linear texture. Linear array of fracture end corresponds to lamellar rank of the fibrils. From the images, the propagation direction of the cracks can be identified. The cracks spread along grain boundaries from one grain to other grains. If planar azimuthal difference between adjacent grains is not too large and forms a small angle grain boundary, linear texture will propagate in a continuous state and extend from one grain to another. If the crack spreads along a wide angle grain boundary, it will propagate in a discontinuous condition.

Figure 4 exhibits the fracture morphologies of T700 from Toray. According to Figure 4(a), T700 also has a grainy and homogeneous cross section similar to those seen in T1 and T300. Compared with T1 and T300, T700 with the diameter of granules in the range of 100-200nm has finer granules that aligned more compactly. From Table 1, T700 has the highest density and tensile strength among the three kinds of carbon fibers, providing evidence that grain refinement can improve tensile strength. The possible reason is as follows. On the one hand, the finer the granules, the higher stacked density and the lower ratio of pore. So, it is easy to achieve compactness and consequently to improve tensile strength. On the other hand, the more the fine granules, the larger areas of grain boundary and the more energy that the crack consumes through grain boundary, this, to some extent, can disturb crack propagation speed.

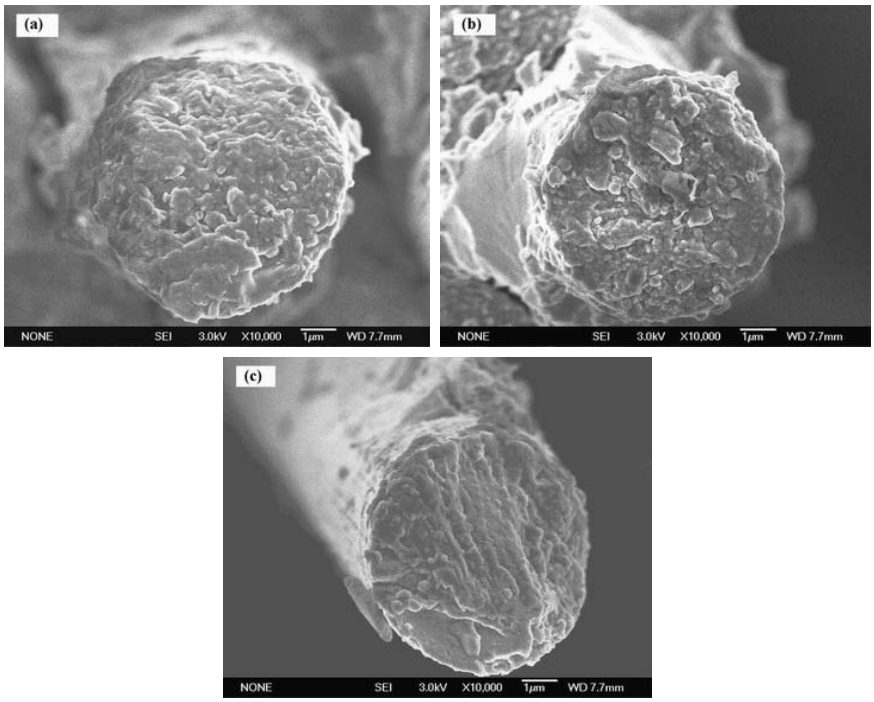

Figure 3 SEM images of the fracture surface of T300

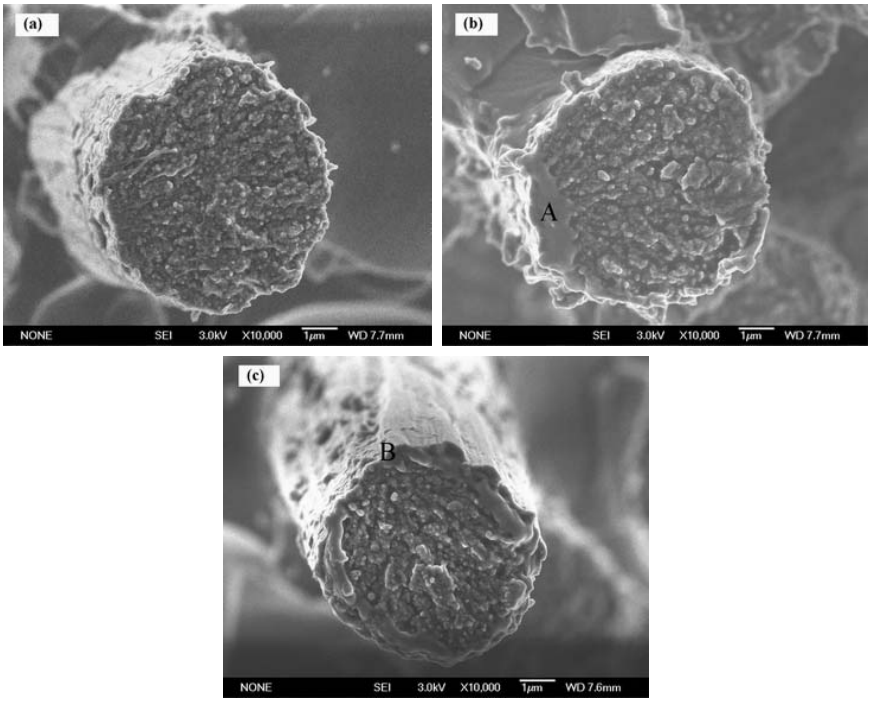

Figure 4 SEM images of the fracture morphology of T700

Besides grainy and homogeneous texture, another texture from the fracture morphology of T700 is shown in Figure 4b and 4c. Beginning from one side (as marked "A" in Figure 4(b) and "B" in Fig. 4(c)), the granules are fanned out in all directions. According to the images, the propagation direction of the cracks can also be identified. The cracks spread in fanlike morphology. There are no indications of sheet-like or skin-core structures in all the specimens.

From Figure 2-4, no evidence for the concept of a thick circumferentially organized sheath surrounding a radially arranged core has been found in our specimens. In addition, from Figure 3 and 4, we can find there are no obvious flaw areas in the fracture surface. So, the flaws are not the only reason for tensile failure. Several mechanisms have been proposed to explain the tensile failure of PAN-based carbon fibers, such as dislocations accumulated at crystallite boundaries [14], stresses on the curved surfaces of the ribbons of graphite planes [15], the presence of three dimensional graphite [16], plastic deformation at crystallite boundaries [17], and Reynolds-Sharp mechanism [18]. Among these failure mechanisms, Reynolds-Sharp mechanism accords with our experimental results as shown in Figure 5-7.

HRTEM analysis of transverse sections

Figure 5-7 are HRTEM images from transverse sections of T1, T300 and T700, respectively. From Figure5-7, we can find within the elliptic region the crystallites have various orientations. According to Reynolds-Sharp mechanism, fiber tensile fracture is initiated due to the large elastic strain energy produced in misoriented crystallites. Misoriented crystallites are the weakest in shear on the basal plane. When a tensile stress is applied parallel to the fiber axis, the shear stress induced parallel to the basal planes can be sufficient to cause basal plane rupture in the misoriented crystallites. The concentration of shear strain energy in the misoriented crystallites is not relieved by the cracks parallel to the layer planes, but by the cracks at right angles. Once formed, a crack will propagate both across the basal plane, and by transference of shear stress, through adjacent layer planes [4, 5, 19].

From HRTEM images, interplanar spacing could be distinguished. According to the images, interplanar spacing of T1, T300 and T700 is 3.434, 3.429 and 3.426Å, respectively, which correspond to (002) plane of PAN-based carbon fibers. The degree of graphitization (P) has been defined by the following empirical equation proposed by Maire and Mering [20]:

$$P = \frac{3.44 - d}{3.44 - 3.354} \times 100\% \qquad (\mathbf{2})$$

where d is the measured interlayer spacing, 3.44Å is the interplanar spacing of disorder carbon material and 3.354Å is the interplanar spacing of single crystal of graphite. Based on the measured value above, T700 has a relatively higher degree of graphitization with 16.3%, whereas T1 and T300 is 7.0% and 12.8% respectively. Above results can be verified further by XRD analysis as shown in Table 1. Figure 8 is XRD pattern of three kinds of PAN-based carbon fibers. Although the values of interplanar spacing have some little differences between XRD and HRTEM, the trend is the same. T700 has the smallest interplanar spacing and the highest degree of graphitization. Besides, from Table 1 it can be seen T700 has the highest crystallinity among three carbon fibers.

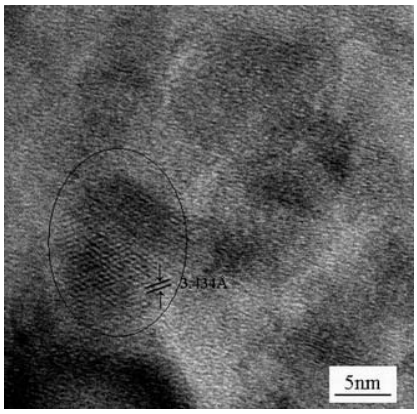

Figure 5 HRTEM image from transverse sections of T1

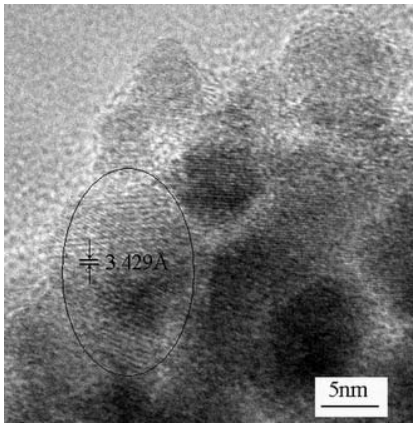

Figure 6 HRTEM image from transverse sections of T300

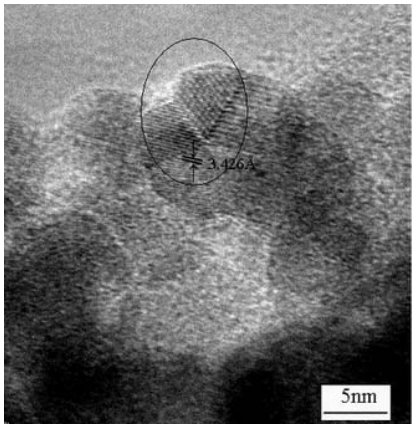

Figure 7 HRTEM image from transverse sections of T700

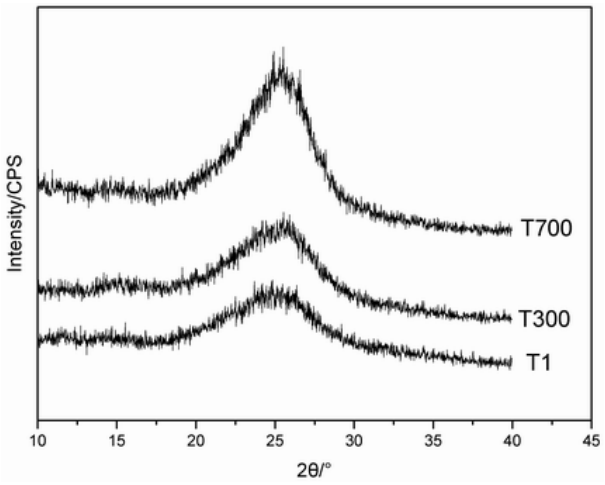

Figure 8 XRD pattern of three kinds of carbon fibers

Conclusion

In this work, SEM provides quantitative information about the fracture morphologies of PAN-based carbon fibers. T1 from our laboratory has homogeneous and granular texture in transverse direction. One void about 1 μm in diameter was found in one fiber center, which decreases its tensile strength. T300 from Toray has rather poorly defined granular and random texture. Apart from randomly distributed grainy morphology, linear texture is found on fracture surface. From the linear direction, the propagation direction of a crack can be easily determined. Similar to T1 and T300, T700 also has a grainy and homogeneous cross section. And, granules distributed in fan-shaped texture are also found on fracture surface. There is no evidence for the thick sheath and the core arrangement suggested by other workers. Misoriented crystallites are also found from HRTEM images in the sections of T1, T300 and T700, which initiate fiber tensile failure. Among three type carbon fibers, T700 has the smallest interplanar spacing, the highest degree of graphitization and the highest crystallinity.

From above discussion, it is certain that only a carbon fiber having minimal defects, high connectivity between the graphitic planes, and high connectivity between the crystallites could bridge the gap between theoretical and practical tensile strength and can improve tensile strength of carbon fibers.

Acknowledgements. This work was financially supported by the National 863 project under grant No. 2002AA304130 and the National Natural Science Foundation of China under grant No. 50673052.

References

1. Donnet JB, Qin RY (1993) Carbon 31: 7.
2. Chand S (2000) J Mater Sci 35:1303.
3. Moreton R, Watt W (1974) Nature 247: 360.
4. Bennett SC, Johnson DJ (1983) J Mater Sci 18: 3337.

5. Zhang WX, Liu J, Wu G (2003) Carbon 41: 2805.
6. Johnson DJ (1987) J Phys D (Appl Phys) 1987 20: 286.
7. Mukesh KJ, Abhiraman AS (1987) J Mater Sci 22: 278.
8. Bai YJ, Wang CG, Lun N, Wang YX, Yu MJ, Zhu B (2006) Carbon 44: 1773.
9. Yu MJ, Wang CG, Bai YJ, Wang YX, Xu Y (2006) Polym Bull 57: 753.
10. Hinrichsen G (1972) J Polym Sci 38: 303.
11. Johson W, Watt W (1967) Nature 215: 384.
12. Guigon M, Oberline A, Desarmot G (1984) Fibre Science and Technology 20: 177.
13. Monthioux M, Bahl OP, Mathur RB (2000) Carbon 38: 475.
14. Cooper GA, Mayer RM (1971) J Mater Sci 6: 60.
15. Stewart M, Feughelman M (1973) J Mater Sci 8: 1119.
16. Coyle RA, Gillin LM, Wicks BJ (1970) Nature 226: 257.
17. Tyson CN (1975) J Phys D (Appl Phys) 8: 749.
18. Reynolds WN, Sharp JV (1974) Carbon 12: 103.
19. Edie DD (1998) Carbon 36: 345.
20. Maire J, Mering J. (1957) In Industrial Carbon and Graphite, Conference of the Society of Chemical Industry, London 204.